Available online at www.CivileJournal.org

Civil Engineering Journal

Vol. 6, No. 8, August, 2020

Estimating the First-year Corrosion Losses of Structural Metals for Continental Regions of the World

Yu. M. Panchenko [a], A. I. Marshakov [a], L. A. Nikolaeva [a], T. N. Igonin [a*]

[a] *A. N. Frumkin Institute of Physical Chemistry and Electrochemistry (IPCE RAS), Russian Academy of Sciences, Moscow, 119071, Russian Federation.*

Received 31 March 2020; Accepted 21 June 2020

Abstract

The knowledge of the first-year corrosion losses of metals (K_1) in various regions of the world is of great importance in engineering applications. The K_1 values are used to determine the categories of atmospheric corrosivity, and K_1 is also the main parameter in models for the prediction of long-term corrosion losses of metals. In the absence of experimental values of K_1, their values can be predicted on the basis of meteorological and aerochemical parameters of the atmosphere using the dose-response functions (DRF). Currently, the DRFs presented in ISO 9223:2012(E) /1/ standard are used for predicting K_1 in any region of the world, along with the unified DRFs /2/ and the new DRFs /3/. The predicted values of corrosion losses (K_1^{pr}) of carbon steel, zinc, copper and aluminum obtained by various DRFs for various continental regions of the world are presented. In this work we used the atmosphere corrosivity parameters and experimental data on the corrosion losses of metals for the first year of exposure (K_1^{exp}) for the locations of the tests performed under the international UN/ECE program, the MICAT project, and the Russian program. For the first time, a comparative assessment of the reliability of various DRFs is given by comparing the values of K_1^{pr} and K_1^{ex} using graphical and statistical methods. The statistical indicators of reliability of predicting the corrosion losses of metals are calculated for various categories of atmosphere corrosivity. It is shown that the new dose-response functions offer the highest reliability for all categories of atmosphere corrosivity.

Keywords: Carbon Steel; Zinc; Copper; Aluminium; Simulation; Atmospheric Corrosion.

1. Introduction

The corrosion losses of metals for the first year of exposure (K_1) are used to determine the category of atmosphere corrosivity toward each metal [1] and for long-term predictions of corrosion mass losses of metals based on models, including the power and power-linear functions. The variability of climatic and aerochemical atmosphere parameters over the years leads to different K_1 values in each test location. Repeated one-year corrosion tests of metals are required to obtain the K_1 values corresponding to the average long-term parameters and the level of atmosphere pollution at a given time. To avoid this, dose-response functions (DRFs) have been developed for estimating K_1 at any location. They are based on long-term average annual atmosphere corrosivity parameters.

The fact that metal corrosion depends on numerous climatic and aerochemical factors of the environment creates great difficulties for the quantitative estimation of the coefficients at the parameters used in DRFs. The coefficients for the main parameters can be obtained from the regularities found by statistical analysis of outdoor or laboratory tests. However, the use of the coefficients obtained for all dependences in DRFs does not ensure the prediction reliability.

* Corresponding author: igonintd@gmail.com

http://dx.doi.org/10.28991/cej-2020-03091563

This is because it is impossible to take the combination of real, continuously changing atmospheric factors into account in DRFs. Therefore, when DRFs are developed, the coefficients determined for at least one or two main parameters can be used. The coefficients for the remaining parameters will not match the pair correlation coefficients.

DRFs can include different atmosphere corrosivity parameters and can have different mathematical forms. Currently, none of the models is perfect. This is, at least, due to the following: a) the mathematical form of DRFs is not quite adequate; b) not all atmosphere corrosivity parameters that affect corrosion are taken into account; c) the values of the coefficients included in the DRFs are inaccurate, etc. In view of this, none of the models that have been developed can give reliable predictions of K_1^{pr} for territories with a wide range of atmosphere corrosivity which corresponds to categories C1-CX according to ISO 9223:2012 [1]. It is possible that each DRF can give reliable K_1^{pr} values only for certain categories of atmosphere corrosivity.

The application of any previously developed DRF for a given territory first requires estimating the reliability of the K_1^{pr} values they provide. The most reliable DRFs can be chosen in two ways:

- Comparison of K_1^{pr} with K_1^{exp} values obtained in a large number of locations or in priority locations of a given territory, which requires a lot of time and is expensive;
- Use of those DRFs which give the most reliable K_1^{pr} for a given category. This requires preliminary information on the DRFs which are the most trustworthy for territories with a certain corrosivity category.

The DRFs presented in the Standard [1], unified DRFs [2] and new DRFs [3, 4] have been developed for territories with a wide variation range of atmosphere corrosivity parameters. The K_1^{pr} values were calculated using various DRFs in previous studies [3, 4]. However, those studies gave no quantitative estimates of the reliability of K_1^{pr} values obtained by different DRFs. This does not allow one to decide which DRF is the best. A quantitative estimation of the reliability of K_1^{pr} is required to make the right choice of the evaluation criterion. The standard determination coefficient R_{st}^2 is used to determine the reliability of predicting the corrosion losses by a DRF. It is calculated from a data array presented in the $y = K_1^{pr}$, $x = K_1^{exp}$ coordinates [5-7]. However, it was shown that the R_{st}^2 coefficient is not recommended for determining the DRF reliability [8]. A number of statistical methods were suggested both for developing DRFs and for estimating the reliability of K_1^{pr} [8-10].

Based on the above considerations, this work includes:

- Analysis of statistical indicators that are used to estimate the properties of DRFs;
- Selection of a statistical indicator for estimating the reliability of the K_1^{pr} which would be most applicable in engineering practice;
- Calculation of K_1^{pr} values for structural metals by all DRFs;
- Assessment of the reliability of K_1^{pr} values of metals by the selected indicator for each category of atmosphere corrosivity;
- Selection of the most reliable DRFs that provide the more reliable K_1^{pr} for each category of atmosphere corrosivity.

The purpose of this work is to estimate the reliability of K_1^{pr} values of these standard metals as calculated by different DRFs for each category of atmosphere corrosivity.

2. Procedure

This study was performed using the climate parameters of atmosphere corrosivity and the results on the first-year corrosion losses of metals in continental test locations K_1^{exp} reported previously [3, 4]. Data for CS, Zn and Cu were taken from the UN/ECE international program [11, 12], data for Cu and Al only were taken from the MICAT project [13, 14], and data for all the metals were taken from the Russian Federation program (RF) [15]. The K_1^{pr} values were calculated for all the metals using the new DRFs [3, 4, 8] (hereinafter DRF^N) and the DRF presented in the standard [1] (hereinafter DRF^S). Calculations by the unified DRFs [2] (hereinafter DRF^U) are given only for carbon steel (CS) and Zn due to the lack of required atmosphere corrosivity parameters used in the equations.

Errors made in the previous study [3, 4] should be noted:

- In K_1^{pr} calculations by DRF^s (except CS for locations under the RF), the recalculation $[SO_2]$ mg/(m^2 day) = $[0.67 \cdot SO_2]$ µg/m^3 was used in accordance with study of Mikhailovskii and Sanko (1979) [16] instead of $[SO_2]$ mg/(m^2 day) = $[0.8 \cdot SO_2]$ µg/m^3 according to ISO 9223:2012(E).
- For steel in the locations covered by the RF program, by mistake, no recalculation was performed for DRF^S and the assumption $[SO_2]$ mg/(m^2 day) = $[SO_2]$ µg/m^3 was used.

This led to an increase in K_1^{pr} values for steel in the locations covered by the RF program and to a slight decrease in K_1^{pr} in all the other cases. In this work, the recalculation of $[SO_2]$ according to ISO 9223:2012(E) standard was used for all locations for consistency.

It should also be reminded that the K_1^{pr} values obtained by DRF^U for steel were increased 7.8-fold like in the previous study [3]. It was based on the assumption that the DRF^U for steel were developed for corrosion losses in μm rather than in g/m^2 according to the assumption made by Tidblad et al. [2].

It should also be noted that DRF^N developed for carbon steel and zinc [3] and for copper [4] were improved using statistical methods of analysis for zinc [8], and in the development of coastal atmospheres DRF for carbon steel and copper [17]. The improvement was achieved by changing the coefficients at T>10 °C (carbon steel, zinc, copper) and Prec (carbon steel, zinc). These changes are justified by the fact that the continental places according to the UN/ECE and RF programs and the MICAT project used for the development of the DRF^N almost never feature high temperatures (T> 10 °C) and have a large amount of precipitation, as was observed in coastal places under the MICAT project. DRF^N remained unchanged for aluminum.

The DRF^N for all the metals are presented by Equations 1 to 4:

For carbon steel

$$\begin{aligned} K&=7.7\cdot[SO_2]^{0.47}\cdot\exp\{0.024\cdot RH+0.095\cdot(T\text{-}10)+0.00035\cdot Prec\} \quad T\le 10^\circ C \\ K&=7.7\cdot[SO_2]^{0.47}\cdot\exp\{0.024\cdot RH-0.065\cdot(T\text{-}10)+0.00035\cdot Prec\} \quad T>10^\circ C \end{aligned} \tag{1}$$

For zinc

$$\begin{aligned} K&=0.45\cdot[SO_2]^{0.36}\cdot\exp\{0.023\cdot RH+0.025\cdot(T\text{-}10)+0.00035\cdot Prec\} \quad T\le 10^\circ C \\ K&=0.45\cdot[SO_2]^{0.36}\cdot\exp\{0.023\cdot RH-0.055\cdot(T\text{-}10))+0.00035\cdot Prec\} \quad T>10^\circ C \end{aligned} \tag{2}$$

For copper

$$\begin{aligned} K&=0.50\cdot[SO_2]^{0.38}\cdot\exp\{0.025\cdot RH+0.085\cdot(T\text{-}10)+0.0003\cdot Prec\} \quad T\le 10^\circ C \\ K&=0.50\cdot[SO_2]^{0.38}\cdot\exp\{0.025\cdot RH-0.055\cdot(T\text{-}10))+0.0003\cdot Prec\} \quad T>10^\circ C \end{aligned} \tag{3}$$

For aluminum

$$\begin{aligned} K&=0.010\cdot[SO_2]^{0.67}\cdot\exp\{0.039\cdot RH+0.032\cdot(T\text{-}10)\text{-}0.0001\cdot Prec\} \quad T\le 10^\circ C \\ K&=0.010\cdot[SO_2]^{0.67}\cdot\exp\{0.039\cdot RH-0.065\cdot(T\text{-}10)\text{-}0.0001\cdot Prec\} \quad T>10^\circ C \end{aligned} \tag{4}$$

3. Results and Discussion

3.1. Statistical Methods for Estimating the DRF Reliability and the K_1^{pr} Accuracy

State standards or international standards exist for any corrosion studies. The use of standards allows the testing, acquisition of meteorological and aerochemical data, processing of samples, and comparison of the results to be performed consistently. There are no established standards for processing large amounts of data with application of statistical tests and for graphical demonstration of results. This leads to difficulties in comparing the results obtained for different experimental data sets or within a single data set. In view of this, it is necessary to consider the statistical methods used by different authors for estimating the DRF reliability and K_1^{pr} accuracy and select at least one of them which is most suitable for practical use.

The experimental first-year corrosion losses (K_1^{exp}), the atmosphere corrosivity parameters and the K_1^{pr} values obtained from DRFs for test locations form a large data array. The choice of atmosphere corrosivity parameters and the estimation of their effects on corrosion are performed using statistical methods. Statistical methods are also used to assess the accuracy of K_1^{pr}.

The standard coefficient of determination R_{st}^2**.** So far, the linear correlation coefficient R_{st} of K_1^{pr} and K_1^{exp} variables are considered to be the main indicator of DRF reliability [18]:

$$R_{st}=\frac{\sum(x_i-x_{av})(y_i-y_{av})}{[\sum(x_i-x_{av})^2\sum(y_i-y_{av})^2]^{\frac{1}{2}}}=\frac{\sum x_iy_i-nx_{av}y_{av}}{[(\sum x_i^2-n(x_{av})^2(\sum y_i^2-n(y_{av})^2)]^{\frac{1}{2}}} \tag{5}$$

Where x_i and y_i are the observed values, x_{av} and y_{av} are their average arithmetic values, and n is the number of observations. To prevent negative R_{st} values, R_{st}^2 is used as the standard coefficient of determination. It is believed that the closer the value of R_{st}^2 to 1, the more reliable the K_1^{pr} values.

This indicator of K_1^{pr} reliability was primarily used in the Standard [1], in the ISOCORRAG report [19] and in a number of other studies, e.g., [11, 20-27], and also for estimating the reliability of corrosion losses over long periods of time [28-30].

It was shown [8] that absolute accuracy of K_1^{pr} was reached if the K_1^{exp} values equaled the K_1^{pr} values. Absolute accuracy of K_1^{pr} for all test locations is graphically represented by the $K_1^{pr} = K_1^{exp}$ line, i.e., the $y = x$ line. Therefore, it is necessary to consider the scatter of points (x_i; y_i) with respect to the $y = x$ line with $a = 1$, $b = 0$ (hereinafter, the bisectrix of the angle between the axes if the x and y axes are plotted using the same scale) [8, 10].

Taking this into account, various DRFs were estimated not by R_{st}^2 but by the generalized coefficient of determination R_{new}^2 indicating the deviation of points (x_i; y_i) from the bisectrix [8]. The generalized coefficient of determination is calculated by Equation 6:

$$R_{new}^2 = 1 - \frac{\sum_{i=1}^{n} (y_i - \frac{(yx)_{av}}{(x^2)_{av}} x_i)^2}{\sum_{i=1}^{n} (y_i - x_i)^2} \quad (6)$$

Where $(yx)_{av} = \frac{1}{n}\sum_{i=1}^{n} y_i x_i$, $(x^2)_{av} = \frac{1}{n}\sum_{i=1}^{n} x_i^2$.

Hence, the standard coefficient of determination R_{st}^2 cannot be recommended for the comparative estimation of DRF reliability [8, 10].

Other statistical indicators were also suggested in ASTM G 16-95 [18]:

a) The ***Mean Absolute Percentage Error*** was used only in a few studies [8, 10], Equation 7:

$$\text{MAPE}(\%) = \frac{1}{n}\sum_{i=1}^{n} \frac{|x_i - y_i|}{|x_i|} \cdot 100 = \delta_{cp} \quad (7)$$

b) The ***Symmetric Mean Absolute Percentage Error***, Equation 8, was used [8]:

$$\text{SMAPE}\ (\%) = \frac{2}{n}\sum_{i=1}^{n} \frac{|x_i - y_i|}{|x_i| + |y_i|} \cdot 100 \quad (8)$$

c) The ***root-mean-square error (RMSE)*** [10], Equation 9:

$$\text{RMSE} = \sqrt{\frac{1}{N}\sum_{n=1}^{N} \left(\overset{\frown}{y}_n - y_n \right)^2} \quad (9)$$

This indicator is used to estimate the mean error expressed in g/m^2 or μm for all test locations. This error should not be large for locations with weakly corrosive atmospheres, but it can be substantially larger for locations with a corrosive environment.

Furthermore, the ***confidence angle Δ of the scatter*** corresponding to the angle of deviation of points (x_i ;y_i) from the bisectrix whose slope is π/4 was considered, Equation 10 [8]:

$$\Delta_i = \left| \arctan \frac{y_i}{x_i} - \pi / 4 \right| \quad (10)$$

In the study by Surnam and Oleti (2012), not only R_{st}^2, but also the maximum Mahalanobis distance was used to choose the DRF for long-term predictions [28]. The smaller the latter parameter is, the more reliable the model. The model that had both a large R_{st}^2 value and a small maximum Mahalanobis distance was selected.

It is desirable to use all the indicators presented above, except for the standard coefficient of determination R_{st}^2, in the development of DRF. These indicators allow one to estimate the proximity of points (K_1^{pr}; K_1^{exp}) to the $K_1^{pr} = K_1^{exp}$ line, excludes the points with significant deviations, and estimate the absolute and relative errors in K_1^{pr} calculations. In DRF development, analysis of the statistical indicators obtained will make it possible to estimate the need to improve them by using various mathematical functions and/or atmosphere corrosivity parameters and by changing the values of DRF coefficients.

The distribution of points (K_1^{exp}; K_1^{pr}) along the straight line $K_1 = K_1^{exp}$ is unimportant for practical purposes. It is important that the error in the calculation of K_1^{pr} values should not exceed certain MAPE relative measurement errors, that is, δ_{av}, Equation 7. Taking into account that a logarithmic distribution is characteristic of corrosion losses [1], it is advisable to calculate the mean relative errors for $y_i > x_i$ (+δ) and for $y_i < x_i$ (-δ):

$$+\delta = \frac{1}{m}\sum_{i=1}^{m}\delta_i \quad \text{and} \quad -\delta = \frac{1}{(n-m)}\sum_{i=1}^{n-m}\delta_i \tag{11}$$

$$\text{where } \delta_i(\%) = [(y_i - x_i)/x_i]100, \tag{12}$$

Where m is the number of points with $\delta_i > 0$.

The values of δ_{av}, +δ and -δ can be used to estimate the safety margin of a metal or to determine the choice of protective means.

ISO 9223:2012(E) standard gives the uncertainty intervals (Table 1). For engineering applications, these uncertainty intervals can be taken as the intervals of permissible relative deviations of K_1^{pr} from the actual corrosion losses (K_1^{exp}). The presented intervals are rather wide, while the interval for +δ is larger than that for -δ. The total uncertainty consists of two components: the uncertainty due to the imperfection of a DRF and the uncertainty in the measurements of environmental parameters and K_1^{exp} values. The uncertainty due to DRF imperfection is predominant. The SMAPE indicator takes the possible errors in the K_1^{exp} values into account. However, assuming in the first approximation that the K_1^{exp} are true values, only the δ_{av} indicator, Equation 7, and the values +δ and –δ, Equation 11, were used to analyze the reliability of K_1^{pr}.

Table 1. Uncertainty range of K_1 prediction according to ISO 9223:2012

Metal	K_1^{pr} error, (calculation by DRF)
CS	From -33% to +50%
Zn	From -33% to +50%
Cu	From -33% to +50%
Al	From -50% to +100%

3.2. Selection of *x* and *y* Variables

Statistical indicators have been developed and are now used in various cases to identify the relationship between random variables that characterize some real processes observed in nature. If R_{st}^2 is used to estimate the reliability of DRF and the accuracy of the K_1^{pr} values obtained, the choice of K_1^{pr} and K_1^{exp} like *x* and *y* variables does not matter. This is due to the fact that R_{st}^2 characterizes only the proximity of the location of (x_i; y_i) points. Therefore, for example, in some publications [11, 19, 20, 27] K_1^{pr} and K_1^{exp} are taken as the *x* and *y* variables, respectively, which is quite acceptable.

If the δ_{av}, +δ and -δ indicators are used, it is necessary to provide a justified choice of *x* and *y* variables. For this purpose, let us compare K_1^{pr} and K_1^{exp} depending on the choice of *x* and *y* variables, using an abstract example. Let K_1^{exp} and K_1^{pr} in test locations A, B, C and D have the values listed in Table 2.

Table 2. Values of K_1^{exp}, K_1^{pr} and δ_i for test locations

Location	K^{ex},	K^{pr},	δ_i ,% at	
	g/m^2		$x = K^{ex}, y = K_1^{pr}$	$x = K^{pr}, y = K^{ex}$
A	30	80	166.7	-62.5
B	150	45	-70.0	233.3
S	260	500	92.3	-48.0
D	550	200	-63.6	175.0

The comparison of K_1^{pr} with K_1^{exp} is graphically represented for two cases: $x = K^{ex}$, $y = K_1^{pr}$ and $x = K^{pr}$, $y = K^{ex}$.

If $x = K^{ex}$ and $y = K_1^{pr}$, the points (K_1^{exp}; K_1^{pr}) corresponding to the test locations are arranged in the order of increasing K_1^{exp} values (Figure 1a). The bisectrix corresponds to the $K_1^{pr} = K_1^{exp}$ line. The absolute error can be estimated by the length of the vertical segment from a point to the bisectrix. One can see that K_1^{pr} have overestimated values in comparison with K_1^{exp} at locations A and C and underestimated values at locations B and D. The relative

errors calculated by Equation 11 range from -63.6% to 166.7%, Table 2. The thin lines in Figure 1a indicate the prediction errors δ_i corresponding to -33% and + 50% in Table 1, as calculated by the equations $K_1^{pr} = 0.67 \cdot K_1^{exp}$ and $K_1^{pr} = 1.50 \cdot K_1^{exp}$, respectively.

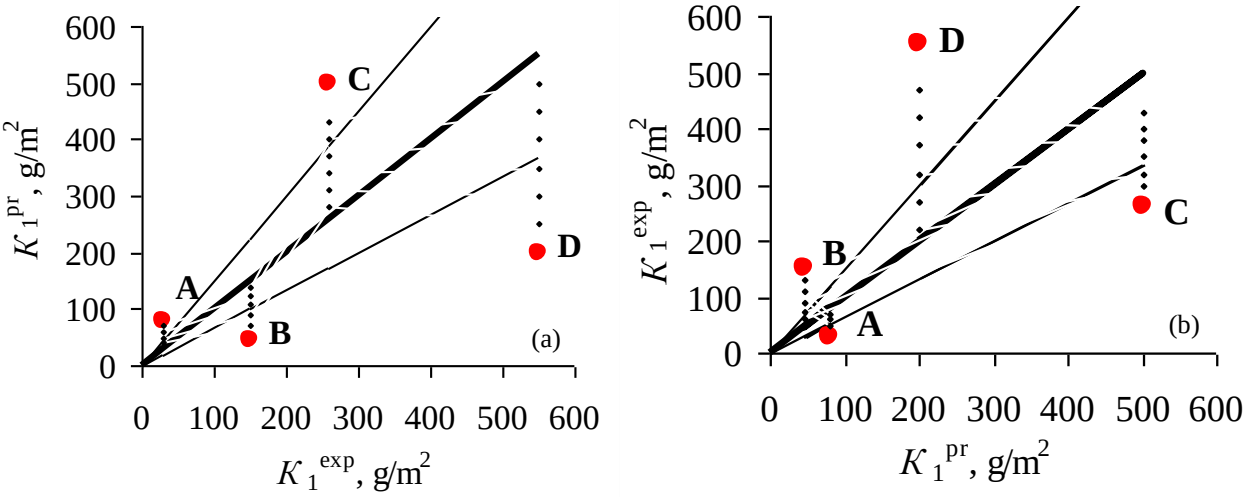

Figure 1. Comparison of K_1^{pr} values with K_1^{exp} for the variables: $x = K^{exp}$, $y = K_1^{pr}$ (a) and $x = K^{pr}$, $y = K^{exp}$ (b). The thin lines designate the prediction errors of -33% and +50%

If $x = K^{pr}$, $y = K^{exp}$, the points (K_1^{pr}; K_1^{exp}) are arranged in the order of increasing K_1^{pr} values (Figure 1b), which is different from their order in Figure 1a. In this case, the lengths of the vertical segments of point deviations from the $K_1^{exp} = K_1^{pr}$ line correspond to the absolute errors of K^{ex} rather than K_1^{pr} , i.e. the K^{exp} - K_1^{pr} differences. The vertical segments for each location are the same in both figures, that is, like in Figure 1a, K_1^{pr} have overestimated values at locations A and C and underestimated values at locations B and D. Hence, the K_1^{pr} values are overestimated for the points located below the bisectrix and underestimated for the points above the bisectix. To draw the lines with relative errors of -33% and + 50%, one has to make recalculations by the equations $K_1^{exp} = 1.49 \cdot K_1^{pr}$ and $K_1^{exp} = 0.67 \cdot K_1^{pr}$, respectively. The relative errors calculated by Eq. (12) for $x = K^{pr}$, $y = K^{exp}$ differ significantly from the δ_i values calculated for $x = K^{exp}$, $y = K_1^{pr}$, both in magnitude and in sign (Table 2). This is due to the fact that in Eq. (12), while the numerators are equal in absolute value, the denominators change from $x = K^{exp}$ to $x = K_1^{pr}$.

The results obtained indicate that the choice of x and y variables significantly affects the calculation of the relative error obtained from Equation 12. In addition, if $x = K_1^{pr}$ is used, the graphical images of the results become inconvenient for the visual assessment of the relative errors.

3.3. Calculation of K_1^{pr} using Different DRF^s

The first-year corrosion losses of metals K_1^{pr} were calculated using DRF^S, DRF^U and DRF^N for the test locations under the UN/ECE, RF programs and the MICAT project [3, 4, 8]. The K_1^{pr} results obtained were presented only in graphical form. Tables 3-6 show the numerical values of K_1^{pr}. These data allow one to estimate the relative error using MAPE (δ_{av}), -δ and +δ indicators.

Table 3. *Carbon steel.* First-year corrosion losses of metals, g/m^2: experimental K_1^{exp} and K_1^{pr} values predicted by different DRFs for test locations under UN/ECE and RF programs

Designation		K_1^{exp}, g/m^2	K_1^{pr} (g/m^2) by			Designation	K_1^{exp}, g/m^2	K_1^{pr} (g/m^2) by		
RF	UN/ECE		DRF^N	DRF^S	DRF^U	UN/ECE		DRF^N	DRF^S	DRF^U
RF1		5.4	11.5	3.9	42.9	FIN6	162.2	112.7	74.8	128.7
RF2		8.1	6.0	1.7	27.3	SPA31	162.2	88.6	111.2	118.7
RF3		12.4	13.4	4.9	39.8	GER7	166.1	122.8	116.9	161.7
RF4		15.2	10.2	3.4	36.7	NL20	172.4	154.5	148.9	171.9
RF5		17.0	15.2	5.2	39.0	US38	176.0	116.4	123.6	124.8
RF6		21.2	23.1	10.1	54.6	NL19	180.2	144.2	134.6	170.9
RF7		23.4	32.6	23.8	76.4	RUS34	181.0	177.8	125.3	133.9
RF8		24.6	24.0	10.5	55.4	US38	184.9	104.6	109.3	110.0
	SPA33	25.7	39.8	45.7	88.7	EST35	185.0	51.3	31.2	109.8

	SPA33	35.9	48.7	62.6	87.5	NOR23	194.0	107.5	41.3	115.1
RF9		36.5	35.9	19.8	78.0	FIN6	195.8	114.5	81.9	128.9
RF10		40.6	42.3	28.7	82.7	NL18	204.4	187.3	166.4	179.2
	SPA33	45.0	63.6	66.3	100.4	NL20	205.1	193.3	197.0	185.7
	FIN5	48.4	47.1	21.9	93.2	GER9	209.8	204.3	201.3	181.4
RF11		49.0	43.2	31.8	83.5	GER8	213.0	232.0	262.6	178.9
	FIN5	59.3	48.9	23.1	98.4	US39	214.0	288.7	342.8	164.6
RF12		63.2	60.7	37.4	90.5	SPA31	222.0	129.9	167.7	130.2
	SWE26	74.9	59.9	39.1	114.0	CS2	224.0	233.3	172.2	158.9
	SWE26	81.1	60.0	41.2	119.3	NOR21	229.0	185.9	139.2	137.4
	GER12	85.0	128.2	69.0	139.6	GER7	230.9	171.2	157.3	171.9
	GER12	89.7	150.9	78.2	145.2	GER9	230.9	225.9	245.3	187.9
	SWE25	95.2	86.4	68.7	120.3	NL18	232.0	228.6	212.0	195.0
	NOR21	100.6	75.4	58.4	108.7	NL19	238.7	193.6	190.4	187.4
	SWE24	103.0	95.4	76.7	123.6	CS1	241.0	303.0	337.9	199.8
	SWE25	103.0	91.4	71.1	114.7	GER11	241.0	238.6	237.1	182.7
	CAN37	103.7	106.1	55.1	120.3	NL20	259.0	238.9	238.4	193.9
	NOR23	109.2	56.4	27.2	97.5	SWE25	263.0	219.1	191.8	167.9
	CAN37	110.0	84.0	38.1	107.6	GER7	264.0	217.1	213.8	184.4
	GER8	116.2	130.8	153.1	131.2	SWE24	264.0	203.8	177.0	164.6
	SWE24	120.1	100.1	78.6	117.6	CS1	270.7	311.0	319.7	182.8
	FIN4	120.9	87.7	54.9	122.3	FIN4	271.0	195.1	138.9	144.9
	RUS34	120.9	163.2	112.6	126.7	FIN6	273.0	222.8	162.3	156.6
	FIN4	130.3	81.0	47.6	115.2	NL19	283.0	236.7	231.9	192.6
	NOR23	131.8	49.6	24.7	92.7	US39	290.2	246.7	289.7	154.9
	FIN5	132.0	115.4	54.1	111.1	GER9	293.0	274.3	289.8	189.6
	GER12	133.0	243.3	150.5	169.3	GER11	293.3	281.9	302.4	200.6
	NOR21	134.9	96.1	86.1	118.6	GER10	294.1	319.0	325.0	199.6
	GER8	141.2	125.6	134.1	128.3	GER11	342.0	316.5	342.3	205.1
	RUS34	141.2	247.0	162.3	145.6	GER10	347.1	362.6	399.9	211.0
	NL18	144.3	161.8	142.2	175.6	CS3	350.2	291.7	326.3	177.5
	SWE26	147.0	99.9	66.0	133.9	CS3	351.8	343.1	399.3	201.7
	CS2	148.2	180.6	130.3	142.3	GER10	373.0	369.8	397.3	197.4
	CAN37	149.0	93.3	52.2	110.8	CS1	438.0	484.4	531.7	229.1
	SPA31	151.3	77.2	102.4	114.4	CS3	557.0	404.6	497.0	206.3
	CS2	152.9	204.0	142.5	141.5					

Table 4. Zinc. First-year corrosion losses of metals, g/m^2: experimental K_1^{exp} and K_1^{pr} values predicted by different DRFs for test locations under UN/ECE and RF programs

Designation		K_1^{exp}, g/m^2	K_1^{pr} (g/m^2) by			Designation	K_1^{exp}, g/m^2	K_1^{pr} (g/m^2) by		
RF	UN/ECE		DRF^N	DRF^S	DRF^U	UN/ECE		DRF^N	DRF^S	DRF^U
RF1		1.64	2.61	2.33	1,83*	NOR21	6.70	4.51	3.87	6.10
	SPA33	1.66	2.41	1.55	4.67	SWE26	6.70	3.60	3.60	5.84
RF4		1.69	2.30	1.62	1,61*	CS2	6.77	8.64	7.56	12.80
RF2		1.81	1.87	1.30	1,19*	CS1	6.98	11.97	14.81	12.66
RF7		2.03	2.88	2.35	3,49*	GER11	7.06	9.58	9.72	10.59
	SPA31	2.30	3.56	3.17	6.40	EST35	7.18	3.05	3.08	4,45*
RF3		2.91	2.66	1.93	1,84*	GER12	7.20	7.56	5.99	6.69
RF5		3.07	3.26	2.52	1,91*	GER12	7.27	8.04	7.32	8.02

	SPA33	3.37	3.18	2.03	5,11*	US39	7.34	9.09	7.72	11.58
	CS2	3.46	7.87	6.84	8.45	GER9	7.63	8.57	9.12	10.24
	NOR21	3.53	3.85	2.92	5.33	FIN5	7.70	3.80	3.43	4.97
	SWE25	3.53	4.46	3.71	6.27	SPA31	7.74	5.37	4.72	7,71*
	SWE25	3.53	4.31	3.77	6.02	CS1	7.78	11.43	12.00	12.18
	SPA31	3.53	4.01	3.41	6.55	GER7	7.85	7.91	9.45	10.13
	GER12	3.74	6.60	5.10	6,21*	GER10	7.85	12.04	13.15	12.49
	SPA33	3.89	4.27	2.96	6.40	NL18	7.92	8.17	8.66	8.99
	SPA33	3.89	2.14	1.38	4.25	CS2	7.99	9.95	10.47	10.13
	GER8	4.10	5.45	4.04	6,92*	NL18	8.14	7.29	7.67	8.89
	GER7	4.25	5.76	6.24	8.04	SWE26	8.31	5.10	5.56	6,10*
	SWE24	4.25	4.65	4.13	6.29	GER12	8.35	10.65	9.09	8,54*
RF9		4.30	3.69	3.12	3,50*	FIN4	8.42	8.40	9.26	8.88
RF11		4.32	3.27	2.33	3,96*	NOR23	8.50	4.42	2.51	6.64
	SWE24	4.54	4.78	4.04	6.51	RUS34	8.64	10.77	10.65	8.65
	FIN5	4.61	3.05	2.75	4.41	FIN5	8.92	5.85	5.26	5,37*
	RUS34	4.61	7.13	6.39	6.84	CS2	8.95	9.66	9.63	8,63*
RF10		4.64	3.45	2.57	3,81*	GER7	9.07	7.48	8.46	9.23
	FIN4	4.68	4.62	4.36	6.16	GER9	9.07	9.04	10.35	10.71
	GER8	4.68	6.09	5.04	8.50	NL19	9.07	7.64	8.92	9.49
	NL18	4.75	7.36	7.41	9.45	FIN6	9.29	8.81	9.81	9.58
	US38	4.75	5.01	3.40	8.09	EST35	9.43	2.68	2.46	4.57
	SPA31	4.82	3.67	2.54	6.11	GER11	9.72	9.80	10.88	11.46
	SWE26	4.90	3.40	3.37	5.38	US38	9.72	4.70	2.99	7.32
	NOR23	5.04	3.41	2.07	5.26	SWE25	9.76	8.96	10.29	9,11*
	FIN4	5.18	4.36	3.89	5.62	CAN37	9.88	4.85	3.78	5,12*
	GER8	5.18	5.50	4.41	7.54	NL18	9.93	9.55	10.56	9,94*
	CAN37	5.26	4.68	3.72	6.22	NL20	10.22	7.13	7.50	9.00
	US39	5.26	9.65	8.80	11.71	RUS34	10.32	7.64	7.48	7,28*
RF6		5.30	3.78	2.50	2,53*	SWE24	10.36	8.47	9.61	8,81*
RF8		5.47	3.83	2.53	2,57*	NOR23	10.58	3.04	1.94	5.02
	FIN6	5.62	5.95	5.17	6.51	GER10	10.66	11.95	13.29	12.45
	SWE25	5.62	5.50	5.59	7.84	US38	10.72	5.19	3.93	6,98*
	CS1	5.69	11.24	13.27	12.01	US39	11.02	10.18	7.47	11.89
	FIN6	5.69	5.53	5.25	6.58	NL19	11.09	8.26	9.28	9.45
	NOR21	5.69	5.53	5.00	7.46	NL20	11.38	8.16	9.25	9.68
	SWE26	6.05	3.41	3.38	5.37	GER11	11.45	10.80	12.55	11.62
	SWE24	6.12	5.53	5.11	7.51	CS3	11.59	13.08	15.68	13.09
	CAN37	6.19	5.52	4.70	6.87	CS3	11.74	10.58	11.72	11.38
	CAN37	6.26	5.34	4.27	6.57	CS3	12.17	12.19	14.55	12.89
	NL20	6.34	6.93	7.33	8.58	US38	12.46	4.75	2.98	7.47
RF12		6.35	5.39	5.09	4,53*	US39	13.61	10.33	9.31	10,50*
	RUS34	6.48	10.10	9.42	8.22	CS1	14.89	16.37	21.20	14,13*
	FIN5	6.62	2.93	2.60	4.12	GER10	15.34	13.05	15.36	12.83
	GER9	6.62	9.74	11.12	11.40	CS3	16.41	13.62	16.67	12.96

DRF^{U}* - calculation of K_1^{pr} without the *Rain*[H^+] parameter

Table 5. Copper. First-year corrosion losses of metals, g/m^2: experimental K_1^{exp} and K_1^{pr} values predicted by different DRFs for test locations under UN/ECE and RF programs and the MICAT project

Designation			K_1^{exp}, g/m^2	K_1^{pr} (g/m^2) by		Designation			K_1^{exp}, g/m^2	K_1^{pr} (g/m^2) by	
MICAT	UN/ECE	RF		DRF^N	DRF^S	MICAT	UN/ECE	RF		DRF^N	DRF^S
		RF2	0.76	0.49	0.14			RF9	6.69	2.47	1.42
PE5			0.80	2.86	1.95	EC1			6.79	2.27	1.38
		RF1	0.84	0.91	0.41	E4			6.79	4.29	1.87
		RF3	0.92	0.98	0.30		GER9		6.93	13.99	9.04
		RF4	0.98	0.79	0.26		NOR21		6.93	8.79	4.1
		RF5	1.37	1.07	0.29	U1			7.05	3.12	2.04
A4			1.43	1.02	0.36	A2			7.23	9.09	3.97
A4			1.52	1.17	0.47	E4			7.41	3.72	1.65
		RF6	1.62	1.61	0.60		FIN4		7.42	8.64	5.04
PE4			1.70	0.89	0.24	M1			7.5	6.97	2.68
A4			1.70	1.16	0.48	E4			7.59	2.26	1.15
		RF8	1.78	1.66	0.62	U1			7.59	3.42	2.31
PE4			1.79	0.78	0.18	U1			7.59	3.21	1.95
M2			2.05	3.42	0.83	E1			7.95	3.03	2.06
		RF12	2.45	3.75	1.88	CO2			8.13	7.54	8.08
M2			2.50	4.44	0.91	A2			8.3	7.63	3.55
		RF11	2.79	2.81	1.39		GER11		9.03	15.87	11.01
		RF7	2.82	2.21	1.18	CO2			9.56	9.61	13.77
	SPA31		3.11	7.08	3.37	E1			9.73	3.25	2.33
EC2			3.21	2.62	1.74	CO2			10.36	5.36	4.01
	SPA33		3.53	3.96	1.93		SWE26		10.67	5.25	4.92
M2			3.57	3.52	0.84		CS1		10.83	21.85	13.73
M3			3.84	4.47	1.63		NOR23		10.93	5.77	3.45
		RF10	4.06	2.79	1.44		GER12		11.38	12.01	7.84
E1			4.11	2.68	1.76		EST35		11.43	2.98	3.3
	RUS34		4.13	7.73	4.05		GER10		11.67	17.62	9.39
M3			4.29	4.21	1.70	A6			11.79	6.82	4.09
M1			4.29	3.57	1.63		FIN5		11.83	5.00	3.01
EC2			4.38	3.32	2.46	U3			11.97	3.69	2.55
	SWE25		4.39	10.41	7.13	B6			12.59	11.49	4.75
E8			4.73	3.90	1.15		NL18		13.33	12.47	10.77
PE6			5.00	2.76	1.85		NL20		13.87	12.81	10.24
	SWE24		5.31	9.82	6.85	B6			14.29	16.84	5.51
M1			5.36	6.36	2.47	A6			14.56	7.35	4.22
E8			5.54	4.78	1.47		CAN37		14.63	4.67	2.88
A2			5.63	6.59	3.22		CS2		14.99	10.64	6.24
B8			5.72	3.82	2.21		US38		15.43	6.63	3.26
	FIN6		5.87	9.93	6.14	A6			15.63	7.71	4.24
EC1			5.89	2.54	1.18		GER7		15.73	11.37	9.05
M3			5.98	4.76	1.17		NL19		16.73	12.72	10.1
	GER8		6.03	12.14	7.95	B6			18.31	14.44	5.12
E8			6.25	4.30	1.29		US39		18.9	13.72	5.56
EC1			6.43	2.71	1.89		CS3		27.5	18.29	9.95

Table 6. Aluminum. First-year corrosion losses of metals, g/m^2: experimental K_1^{exp} and K_1^{pr} values predicted by different DRFs for test locations under the MICAT project and the RF program

Designation		K_1^{exp}, g/m^2	K_1^{pr} (g/m^2) by		Designation		K_1^{exp}, g/m^2	K_1^{pr} (g/m^2) by	
MICAT	RF		DRF^N	DRF^S	MICAT	RF		DRF^N	DRF^S
PE4		0.027	0.028	0.018		RF6	0.280	0.273	0.131
PE4		0.027	0.023	0.016		RF12	0.285	0.612	0.195
PE5		0.027	0.111	0.047		RF9	0.285	0.279	0.148
PE6		0.027	0.081	0.039	E1		0.297	0.129	0.054
U1		0.027	0.102	0.046	E4		0.297	0.291	0.162
U1		0.027	0.098	0.045	M2		0.297	0.170	0.130
U1		0.054	0.110	0.048		RF7	0.310	0.228	0.143
PE5		0.081	0.111	0.047	A6		0.324	0.404	0.193
EC1		0.081	0.137	0.081	E8		0.324	0.288	0.172
EC1		0.081	0.150	0.075	A6		0.351	0.402	0.190
PE6		0.108	0.084	0.041	E1		0.378	0.136	0.056
A4		0.108	0.042	0.024	E1		0.378	0.117	0.050
U3		0.108	0.114	0.050	M2		0.378	0.136	0.098
E4		0.135	0.226	0.123	E8		0.378	0.298	0.175
A4		0.162	0.043	0.024	A2		0.378	0.474	0.253
	RF4	0.164	0.165	0.098	A4		0.405	0.035	0.021
	RF1	0.177	0.227	0.109	A2		0.405	0.430	0.225
	RF2	0.189	0.140	0.084	CO2		0.432	0.377	0.111
	RF8	0.205	0.275	0.133	M1		0.432	0.475	0.269
E4		0.216	0.104	0.053		RF5	0.474	0.345	0.123
E8		0.216	0.280	0.170	A6		0.54	0.471	0.230
A2		0.216	0.443	0.231	CO2		0.648	0.255	0.086
M1		0.216	0.549	0.310	M2		1.242	0.141	0.102
	RF3	0.242	0.223	0.111	B6		1.242	1.218	0.710
	RF11	0.258	0.219	0.149	B6		1.458	1.455	0.919
	RF10	0.259	0.236	0.150	B6		1.836	1.444	0.893

3.4. Estimating the reliability of K_1^{pr} for all test locations

The relative errors δ_{av}, -δ and +δ calculated by Equations 7 and 11 based on the K_1^{exp} and K_1^{pr} data, Tables 3-6, are presented in Table 7.

Table 7. The average relative K_1 prediction errors (δ_{av}, -δ, +δ, %) for DRF^N, DRF^S, and DRF^U for all test locations

Metal	DRF^N			DRF^S			DRF^{U*}		
	δ_{av}	-δ	+δ	δ_{av}	-δ	+δ	δ_{av}	-δ	+δ
St3	23.7	-20.6	31.2	33.6	-35.9	25.2	54.0	-26.2	103.5
Zn	27.7	-25.6	28.9	31.7	-33.0	29.9	39.0	-21.7	44.3
Cu	46.8	-35.7	58.0	58.9	-61.4	40.0	-	-	-
Al	56.4	-33.2	85.7	51.1	-52.3	43.4	-	-	-

DRF^{U*} - for zinc, the test locations where the *Rain*[H^+] parameter was unavailable were not taken into account.

The mean absolute values of δ_{av} for K_1^{pr} calculated by all the DRFs are in the ranges of 23.7-54.0%, 27.7-39.0%, 46.8-58.9% and 51.1- 56.4% for steel, Zn, Cu and Al, respectively. It should be reminded that the K_1^{pr} values calculated by DRF^U for Cu and Al were not considered. The results obtained show that the δ_{av} of K_1^{pr} predictions made using different DRFs have rather close values, except for steel. Therefore, we can assume that all DRFs can be used to calculate K_1^{pr}. However, the $|\delta_{av}|$ values obtained cannot indicate whether the K_1^{pr} values are under/overestimated. Therefore, it is advisable to consider the relative prediction errors separately for K_1^{pr} values which are underestimated (-δ) and overestimated (+δ) in comparison with K_1^{exp}, Table 7. Comparison of the results on -δ, + δ with the

uncertainty intervals ±δ according to the Standard, Table 1, indicates that the -δ and +δ values obtained for all the DRFs are within the uncertainty intervals, except for +δ for steel based on DRF^U (103.5%), for Cu (58.0%) and Al (85.7%) based on DRF^N, as well as -δ for Cu (-61.4%) based on DRF^S. It can be assumed that DRF^N, DRF^S and DRF^U can be used for K_1 predictions, except for the exceptions indicated above. No rejection of test locations was carried out, so significant outliers (K_1^{exp}; K_1^{pr}) for certain test locations due to various reasons can significantly affect the -δ and +δ values.

3.5. Estimation of K_1^{pr} Reliability for Test Locations with Different Categories of Atmosphere Corrosivity

It is stated in ISO 9223:2012(E) standard that the uncertainty of K_1 predictions is the smallest in the medium range of K_1^{exp} values corresponding to atmosphere corrosivity category C3 but it is much higher for territories with atmosphere corrosivity of categories C1 and C5. For category CX, the uncertainties of K_1 prediction are the highest, therefore, predictions of K_1 using the developed DRFs may be unreliable for areas with this category of atmosphere corrosivity.

The C2 category is divided into three additional subcategories in Russia: C2-1, C2-2 and C2-3 (Table 8) [31]. In view of this, let us consider the values of +δ, -δ and δ_{av} for each category, including the additional C2 subcategories (Table 9).

Table 8. Additional C2 subcategories of atmosphere corrosivity suggested for the territory of Russia

Corrosivity category		First-year corrosion losses of metals, K_1				
		Units	Carbon steel	Zinc	Copper	Aluminum
C2	C2-1	g/m²	$10 < K_1 \le 50$	$0.7 < K_1 \le 1.5$	$0.9 < K_1 \le 1.5$	$K_1 \le 0.2$
		μm	$1.3 < K_1 \le 6.4$	$0.1 < K_1 \le 0.21$	$0.1 < K_1 \le 0.17$	-
	C2-2	g/m²	$50 < K_1 \le 100$	$1.5 < K_1 \le 3.0$	$1.5 < K_1 \le 3.0$	$0.2 < K_1 \le 0.35$
		μm	$6.4 < K_1 \le 12.8$	$0.24 < K_1 \le 0.42$	$0.17 < K_1 \le 0.34$	-
	C2-3	g/m²	$100 < K_1 \le 200$	$3.0 < K_1 \le 5$	$3.0 < K_1 \le 5$	$0.35 < K_1 \le 0.6$
		μm	$12.8 < K_1 \le 25$	$0.42 < K_1 \le 0.7$	$0.34 < K_1 \le 0.6$	-

Comparisons of K_1^{pr} values calculated by all DRFs *versus* K_1^{exp} are presented in Figures 2 to 5. To compare the reliability of K_1^{pr} values for locations with different corrosivity, the coordinate field is divided into categories of atmosphere corrosivity determined from the K_1^{exp} values. One can see that for all the metals, the equality $K_1^{pr} = K_1^{exp}$ is observed only in a small number of test locations for each DRF. In most cases, the K_1^{pr} values are over/underestimated relative to K_1^{exp}, which corresponds to the location of points above/below the line of absolute match, $K_1^{pr} = K_1^{exp}$. Some of the points fall outside the limit lines corresponding to the relative errors of -33% and +50% for steel, zinc and copper, as well as -50% and +100% for aluminum.

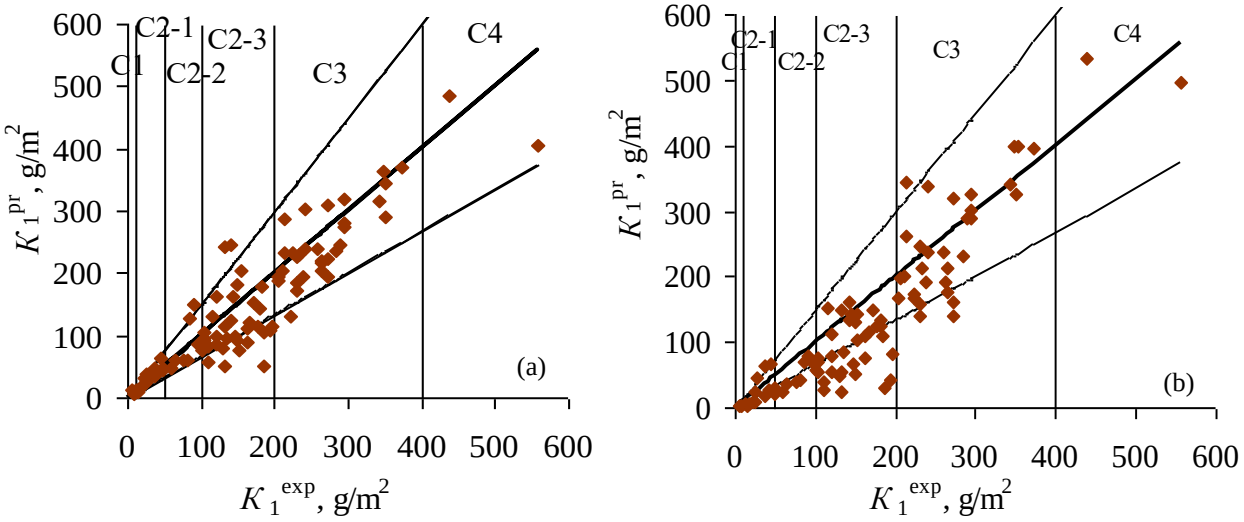

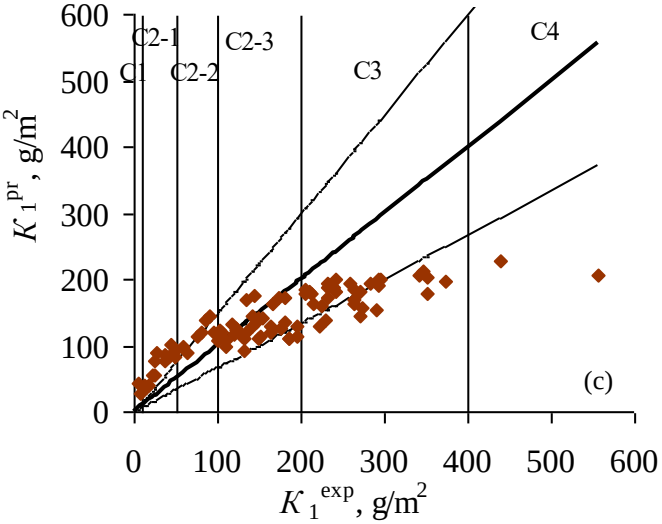

Figure 2. ***Carbon steel.*** **UN/ECE and RF programs. Comparison of K_1^{pr} and K_1^{exp} for test locations with corrosivity categories C1–C4 determined from the K_1^{exp} values. The K_1^{pr} values were calculated by DRF^N (a), DRF^S (b) and DRF^U (c). The thick line is the K_1^{pr} = K_1^{exp} line; the thin lines are the lines of K_1^{pr} relative errors of +50% and -33%**

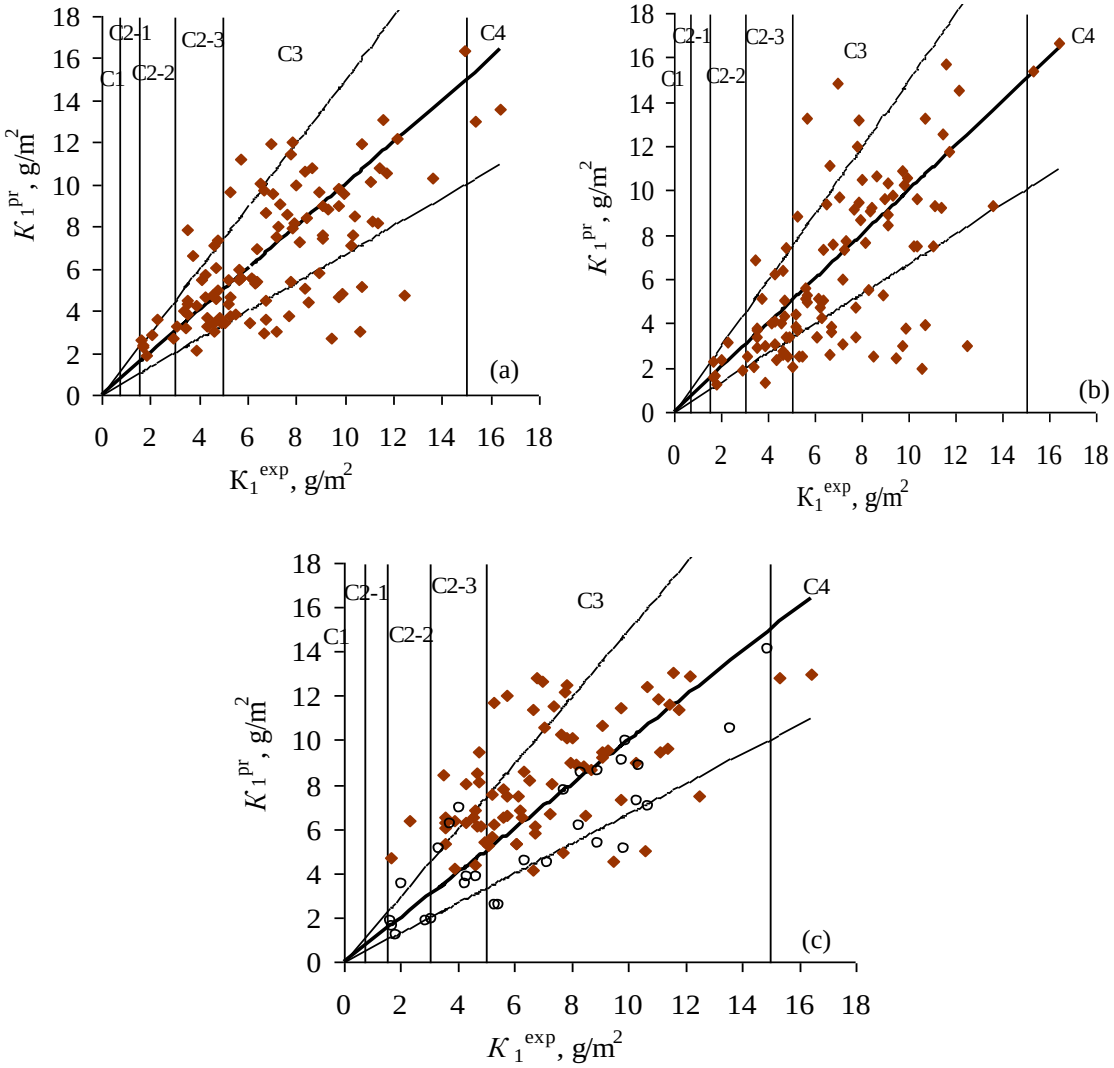

Figure 3. Zinc. UN/ECE and RF programs. Comparison of K_1^{pr} with K_1^{exp} for test locations with corrosivity categories C2-2–C4 determined from the K_1^{exp} values. The K_1^{pr} values were calculated by DRF^N (a), DRF^S (b) and DRF^U (c). ◊ - results on K_1^{pr} for test locations where no *Rain*[H$^+$] parameter is available, only for DRF^U. The thick line is the K_1^{pr} = K_1^{exp} line; the thin lines are the lines of K_1^{pr} relative errors of +50% and -33%

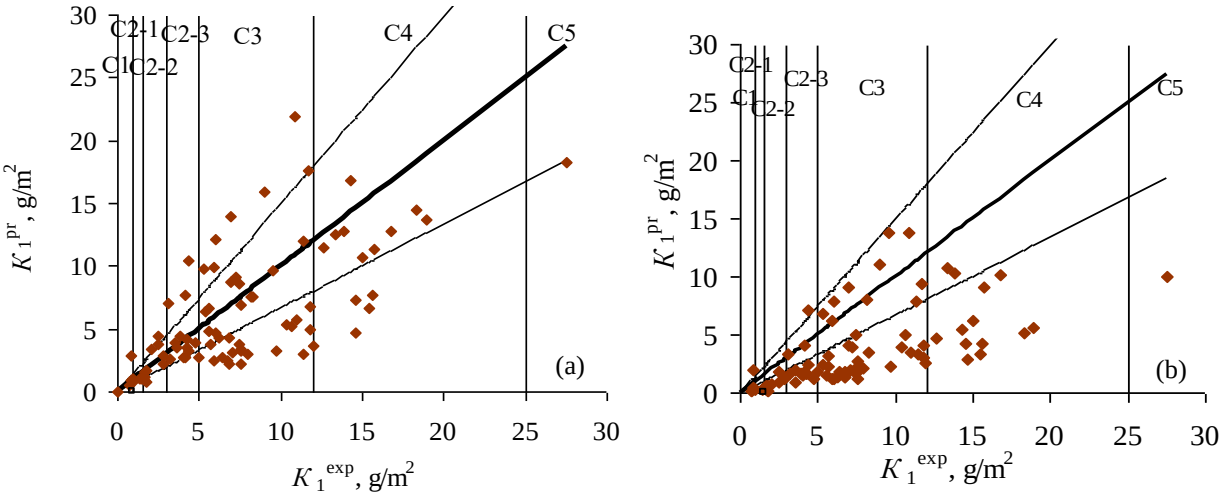

Figure 4. Copper. UN/ECE, RF programs and MICAT project. Comparison of K_1^{pr} with K_1^{exp} for test locations with corrosivity categories C1–C5 determined from K_1^{exp} values. The K_1^{pr} values were calculated by DRF^N (a) and DRF^S (b). The thick line corresponds to $K_1^{pr} = K_1^{exp}$; the thin lines are the lines of K_1^{pr} relative errors of +50% and -33%

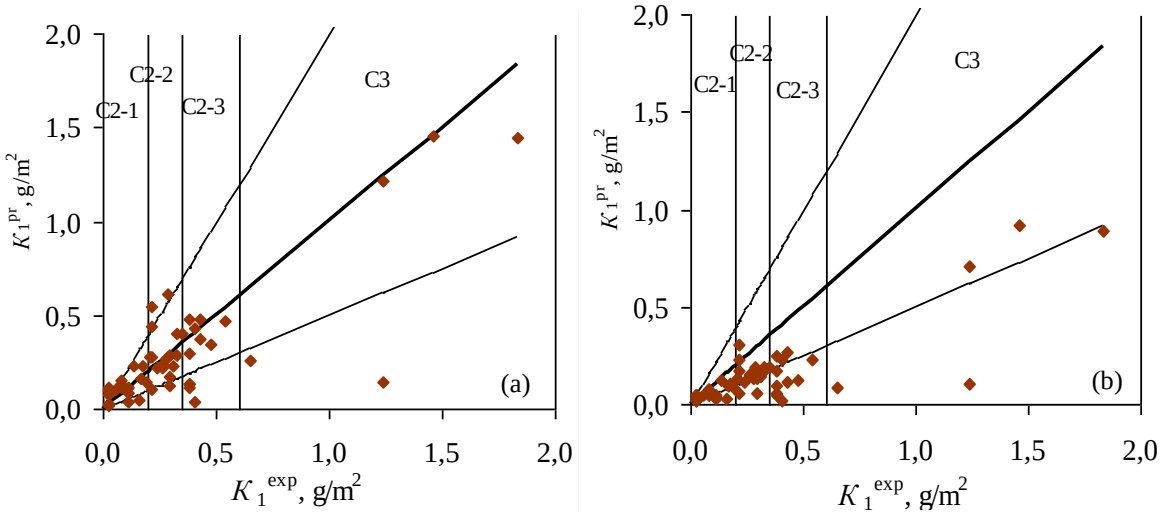

Figure 5. Aluminum. MICAT project and RF program. Comparison of K_1^{pr} with K_1^{exp} for test locations with corrosivity categories C2-1–C3 determined from K_1^{exp} values. The K_1^{pr} values were calculated by DRF^N (a) and DRF^S (b). The thick line corresponds to $K_1^{pr} = K_1^{exp}$; the thin lines are the lines of K_1^{pr} relative errors of +100% and -50%

Table 9 gives an estimate of the relative errors –δ, +δ, and δ_{av} of K_1^{pr} values for each corrosivity category.

Table 9. Average relative errors of K_1^{pr} ($+\delta_{av}$, $-\delta_{av}$ and $|\delta_{av}|$, %) for *n* test locations in each category of atmosphere corrosivity

Metal	Categories	C1		C2-1		C2-2		C2-3		C3		C4		C5	
	DRF	*n*	$\pm\delta_{av}$, $\lvert\delta_{av}\rvert$	*n*	$\pm\delta_{av}$, $\lvert\delta_{av}\rvert$	*n*	$\pm\delta_{av}$, $\lvert\delta_{av}\rvert$	*n*	$\pm\delta_{av}$, $\lvert\delta_{av}\rvert$	*n*	$\pm\delta_{av}$, $\lvert\delta_{av}\rvert$	*n*	$\pm\delta_{av}$, $\lvert\delta_{av}\rvert$	*n*	$\pm\delta_{av}$, $\lvert\delta_{av}\rvert$
St3	DRF^N	1	-25.6	9	-10.3	4	-15.4	24	-28.4	12	-12.8	1	-27.4	-	-
		1	+113.5	4	+27.5	3	+59.5	10	+34.5	19	+14.5	1	+10.6	-	-
		2	69.6	13	19.5	7	28.0	34	31.6	31	13.2	2	19.0	-	-
	DRF^S	2	-53.4	9	-53.6	7	-36.9	31	-41.1	20	-18.9	1	-10.7	-	-
		-	-	4	+50.3	-	-	3	+20.0	11	+17.9	1	+21.4	-	-
		2	53.4	13	52.6	7	36.9	34	39.3	31	18.6	2	16.1	-	-
	DRF^U	-	-	-	-	-	-	24	-17.9	31	-30.8	2	-55.3	-	-
		2	+462.7	13	+145.6	7	+51.6	10	+12.7	-	-	-	-	-	-
		2	462.7	13	145.6	7	51.6	34	16.4	31	30.8	2	55.3	-	-

Zn	DRF^N	-	-	-	-	1	-8.6	9	-23.0	45	-26.9	2	-15.9	-	-
		-	-	-	-	6	+40.1	16	+32.5	27	+26.5	-	-	-	-
		-	-	-	-	7	35.6	25	29.1	72	26.7	2	15.9		-
	DRF^S	-	-	-	-	4	-18.1	17	-26.7	43	-34.8	-		-	-
		-	-	-	-	3	+31.7	8	+36.9	30	+30.8	2	+0.9	-	-
		-	-	-	-	7	23.9	25	30.0	72	33.1	2	0.9	-	-
	DRF^{U*}	-	-	-	-	-	-	1	-4.3	16	-22.2	1	-18.6	-	-
		-	-	-	-	2	+180.0	17	+61.9	40	+30.0	-	-	-	-
		-	-	-	-	2	180.0	18	58.7	56	28.1	1	18.6	-	-
Cu	DRF^N	1	-35.3	3	-23.3	7	-26.8	9	-21.2	26	-46.5	12	-31.4	1	-33.5
		2	132.9	1	+6.5	4	+49.6	5	+76.1	14	+49.8	1	17.8	-	-
		3	100.4	4	19.1	11	35.0	14	40.8	40	47.6	13	30.4	1	33.5
	DRF^S	2	-66.4	4	-73.6	11	-63.7	12	-54.5	33	-62.6	13	-58.1	1	-63.8
		1	+143.8	-	-	-	-	2	+35.0	7	+26.6	-	-	-	-
		3	92.2	4	73.6	11	63.7	14	51.8	40	56.3	13	58.1	1	63.8
Al	DRF^N	-	-	5	-39.9	11	-20.7	8	-45.3	5	-34.6	-	-	-	-
		-	-	13	+111.8	6	+77.0	4	+14.0	-	-	-	-	-	-
		-	-	18	91.8	17	40.5	12	34.6	5	34.6	-	-	-	-
	DRF^S	-	-	13	-42.6	15	-48.6	12	-63.4	5	-61.9	-	-	-	-
		-	-	5	+50.7	2	+25.1	-	-	-	-	-	-	-	-
		-	-	18	44.9	17	45.8	12	63.4	5	61.9	-	-	-	-

DRF^{U*} - for zinc, the test locations where the $Rain[H^+]$ parameter was unavailable were not taken into account.

Carbon steel. The atmosphere corrosivity toward carbon steel at test locations as determined from K_1^{exp} falls within categories C1-C4. For the K_1^{pr} values calculated by DRF^N, the values of -δ and +δ fall within the specified interval for all categories except for categories C1 and C2-2: +δ = 124.1% and + 63.2% for one and three test sites, respectively. For SRF^S, the -δ values fall beyond the lower limit of the range for categories P1 and P2, but for categories P3 and P4, the -δ and +δ values do not fall beyond the specified range, as one can clearly see in Figure 2b. The K_1^{pr} values based on DRF^U are more unreliable: they are extremely overestimated for categories C1, C2-1 and C2-2 (the +δ values range from 51.6 to 462.7%) but underestimated for category C4 (-δ = -55.3%). The most reliable K_1^{pr} values are only provided for subcategory C2-3, Figure 2c.

For *zinc*, the atmosphere corrosivity at the test location ranges from C2-2 to C4. For all the DRFs, the deviation of points from the $K_1^{pr} = K_1^{exp}$ line is observed for a large number of locations, Figure 3. Some of the points fall outside the relative error range from –33% to +50%. Outside this range, the points for DRF^N are located symmetrically relative to the $K_1^{pr} = K_1^{exp}$ line, mostly below the line for the DRF^S and mostly above it for DRF^U, taking into account that for certain test locations, the hydrogen ion concentration in precipitation, $Rain[H^+]$, was not taken into account in the K_1^{pr} calculations. However, despite the scatter of points, the mean values of –δ and +δ correspond to the relative error range from -33% to +50% in all the corrosivity categories for DRF^N and DRF^S, and for DRF^U only in categories C3 and C4.

The corrosion testing of *copper* under the UN/ECE program and the MICAT project was carried out in a significantly smaller number of locations than that of steel and zinc. Considering that the corrosivity categories range from C1 to C5, the number of test locations in each of them is small. Therefore, considerable deviations of individual points can significantly affect the -δ and +δ values, for example, in category C1 for DRF^N and DRF^S, Table 5. In the other categories, the values of -δ and +δ for DRF^N are within the relative error interval from -33% to +50%, except for categories C2-3, where the +δ is +76.13%. In contrast to DRF^N where the scatter of points is symmetrical with respect to the $K_1^{pr} = K_1^{exp}$ line, for DRF^S the points are mainly located below this line, Figure 4. As a result, the -δ values are well below the -33% limit for all the categories.

The corrosion tests of *aluminum* were carried out only under the MICAT project in a small number of locations and under the RF program, therefore the total number of locations is as small as 52. For certain test locations under the MICAT project, the K_1^{exp} values were only 0.027, 0.054 and 0.081 g/m^2, Table 6. Due to the absence of the upper limit for category C1 in the Standard [1], category C2-1 was assigned for those places as the smallest one where $K_1^{exp} \leq 0.2$ g/m^2 in accordance with the Standard. According to K_1^{exp}, the corrosivity category for all the locations was only C2 with additional subcategories (Table 8) or C3. For DRF^N, the arrangement of points relative to the $K_1^{pr} = K_1^{exp}$ line is

rather symmetrical, but for DRF^S, the values of K_1^{pr} generally have underestimated values in comparison with K_1^{exp}, Figure 5. It can also be seen from Figure 5 that the point with the (K_1^{exp} = 1.24 g/m^2; K_1^{pr} = 0.10 g/m^2) coordinates is apparently an outlier. Despite the scatter of points, the -δ and +δ values for DRF^N correspond to the relative error range from -50% to +100% in all the categories, even taking into account the assumed outlier point, except for category C2-1 where +δ = 111.8% that is not much higher than the upper relative error value. The overestimated K_1^{pr} values are primarily due to the complexity of accurate simulation of extremely small K_1^{exp} values for which +δ = +111.8% is not so significant. Unlike DRF^N, the K_1 values based on DRF^S for category C2-1 and C2-2 are quite reliable, which is, in general, due to the underestimation of K_1^{pr} values for all the categories (Figure 5); -δ and +δ correspond to the relative error range of -50% to +100%, respectively. However, for categories C2-3 and C3 there are only underestimated K_1^{pr} values compared to K_1^{exp} with -δ = -63.4 and -61.9%, respectively.

The value of the relative error δ_{av} for each category of atmosphere corrosivity (Table 5) provides incomplete information on how much the K_1^{pr} values differ from K_1^{exp}: whether K_1^{pr} values are overestimated or underestimated, and what measures should be taken to protect structures from corrosion in practice based on DRF results.

The results obtained from comparing the K_1^{pr} values calculated by different DRFs with K_1^{exp} indicate that an absolute equality of K_1^{pr} and K_1^{exp} is unlikely for any test site. The relative errors -δ and +δ for each category are averages of scattered points, and the smaller their values, the greater the probability that K_1^{pr} can be obtained for any test site within the relative errors provided. The -δ and +δ values indicate that the most reliable K_1^{pr} can be obtained:

- For carbon steel, using DRF^N for locations with all corrosivity categories; using DRF^S – for places with corrosivity categories C2-3, C3 and C4; and using DRF^U – only for categories C2-3 and C3;
- For zinc, using DRF^N and DRF^S for test locations with corrosivity C2-2, C2-3, C3 and C4, and using DRF^U – only for categories C3 and C4;
- For copper, only using DRF^N for test locations with corrosivity from C1 to C5, although this model can give overestimated K_1^{pr} values for C2-2 and C2-3 categories, whereas DRF^S will mostly give significantly underestimated K_1^{pr} values for all categories;
- For aluminum, only using DRF^N for test sites with corrosivity C2-1, C2-2, C2-3 and C3, and using DRF^S – only for categories C2-1 and C2-2.

4. Conclusions

- Various statistical indicators characterizing the properties of dose-response functions and the need to use these indicators to estimate the reliability of predicting the corrosion losses of metals have been considered. It has been shown that to estimate the reliability of K_1^{pr} values calculated by DRFs, it is advisable to use the MAPE indicator to find the average relative errors and the –δ and +δ values that characterize underestimated and overestimated K_1^{pr} values in each category of atmosphere corrosivity, taking into account the uncertainty range of corrosion loss predictions in accordance with ISO 9223:2012(E).
- The values of first-year corrosion losses of standard metals were first calculated by three types of dose-response functions (DRF^S, DRF^U and DRF^N) for various continental regions of the world. Based on the large data array of K1pr and experimental K1exp values thus obtained, the MAPE index, -δ and + δ values were calculated.

It has been found that reliable K_1^{pr} can be obtained with higher probability:

- For carbon steel: using DRF^N for all corrosivity categories, using DRF^S - for locations with corrosivity categories C2-3, C3 and C4, and using DRF^U - only for categories C2-3 and C3;
- For zinc: using DRF^N and DRF^S for all the atmosphere corrosivity categories listed where tests were carried out, i.e., C2-2, C2-3, C3 and C4, and using DRF^U, only for categories C3 and C4;
- For copper: only using DRF^N;
- For aluminum: using DRF^N for test sites with corrosivity C2-1, C2-2, C2-3 and C3, and using DRF^S, only for categories C2-1 and C2-2.

5. Conflicts of Interest

The authors declare no conflict of interest.

6. References

[1] ISO 9223:2012. Corrosion of Metals and Alloys — Corrosivity of Atmospheres — Clasification, Determination and Estimation, 2nd ed.; International Organization for Standardization: Geneva, Switzerland, 2012.

[2] Tidblad, J., Mikhailov, A. A., Kucera, V. "Unified Dose-Response Functions after 8 Years of Exposure. Quantification of Effects of Air Pollutants on Materials", UN ECE Workshop Proceedings, Umweltbundesamt, Berlin. 1999: 77–86.

[3] Panchenko, Yulia, and Andrey Marshakov. "Prediction of First-Year Corrosion Losses of Carbon Steel and Zinc in Continental Regions." Materials 10, no. 4 (April 18, 2017): 422. doi:10.3390/ma10040422..

[4] M. Panchenko, Yulia, Andrey I. Marshakov, Ludmila A. Nikolaeva, and Victoria V. Kovtanyuk. "Prediction of First-Year Corrosion Losses of Copper and Aluminum in Continental Regions." AIMS Materials Science 5, no. 4 (2018): 624–649. doi:10.3934/matersci.2018.4.624.

[5] Hao, Long, Sixun Zhang, Junhua Dong, and Wei Ke. "Atmospheric Corrosion Resistance of MnCuP Weathering Steel in Simulated Environments." Corrosion Science 53, no. 12 (December 2011): 4187–4192. doi:10.1016/j.corsci.2011.08.028.

[6] Leuenberger-Minger, A.U., B. Buchmann, M. Faller, P. Richner, and M. Zöbeli. "Dose–response Functions for Weathering Steel, Copper and Zinc Obtained from a Four-Year Exposure Programme in Switzerland." Corrosion Science 44, no. 4 (April 2002): 675–687. doi:10.1016/s0010-938x(01)00097-x.

[7] Pei, Zibo, Dawei Zhang, Yuanjie Zhi, Tao Yang, Lulu Jin, Dongmei Fu, Xuequn Cheng, Herman A. Terryn, Johannes M.C. Mol, and Xiaogang Li. "Towards Understanding and Prediction of Atmospheric Corrosion of an Fe/Cu Corrosion Sensor via Machine Learning." Corrosion Science 170 (July 2020): 108697. doi:10.1016/j.corsci.2020.108697.

[8] Panchenko, Yu. M., A. I. Marshakov, I. V. Bardin, and A. V. Shklyaev. "Use of Statistical Analysis Methods for Estimating the Reliability of First-Year Carbon Steel and Zinc Corrosion Loss Predictions Calculated Using Dose-Response Functions." Protection of Metals and Physical Chemistry of Surfaces 55, no. 4 (July 2019): 753–760. doi:10.1134/s2070205119040142.

[9] Nikitin, Evgeny, Georgy Shumatbaev, Dmitriy Terenzhev, Kirill Sinyashin, and Egor Rastergaev. "New Sintanyl Phosphonates for Protection of Oil and Gas Pipelines from Steel Corrosion." Civil Engineering Journal 5, no. 4 (April 27, 2019): 789–795. doi:10.28991/cej-2019-03091288.

[10] Zhi, Yuanjie, Dongmei Fu, Dawei Zhang, Tao Yang, and Xiaogang Li. "Prediction and Knowledge Mining of Outdoor Atmospheric Corrosion Rates of Low Alloy Steels Based on the Random Forests Approach." Metals 9, no. 3 (March 26, 2019): 383. doi:10.3390/met9030383.

[11] Tidblad, J., Kucera, V., Mikhailov, A. A. "Statistical analysis of 8 year materials exposure and acceptable deterioration and pollution levels". UN/ECE ICP on Effects on Materials, Report No. 30, Stockholm, Sweden: Swedish Corrosion Institute. 1998: 1-49.

[12] Tidblad, J., Kucera, V., Mikhailov, A. A., Henriksen, J., Kreislova, K., Yaites, T., Stöckle, B., Schreiner, M. "UN ECE ICP Materials. Dose-response functions on dry and wet acid deposition effects after 8 years of exposure". Water, Air, and Soil Pollution.130 (2001): 1457-1462.

[13] Morcillo, M., Almeida, E. M., Rosales, B. M., et al. "Functiones de Dano (Dosis/Respuesta) de la Corrosion Atmospherica en Iberoamerica". Corrosion y Proteccion de Metales en las Atmosferas de Iberoamerica, Madrid, Spain: Programma CYTED.1998. P. 629–660.

[14] Morcillo, M. "Atmospheric corrosion in Ibero-America: The MICAT project". Atmospheric corrosion, ASTM STP 1239, Philadelphia, PA: American Society for Testing and Materials. 1995: 257–275.

[15] Panchenko, Yu. M., Shuvakhina, L. N., Mikhailovskii, Yu. N. "Atmospheric corrosion of metals in Far Eastern regions". Zashchita Metallov. 1982;18: 575–582 (In Russian).

[16] Mikhailovskii, Yu.N., Sanko, A.P. "Statistical estimation of sulphur dioxide concentration oscillation effect in atmosphere on metal corrosion rate". Zashchita Metallov. 1979. Vol. 15. P. 432–437 (In Russian).

[17] Panchenko, Yu. M., Marshakov, A. I., Nikolaeva, L. A., Igonin, T. N. "Development of models for the prediction of first-year corrosion losses of standard metals for territories with coastal atmosphere in various climatic regions of the world". 2020 (in print - Corrosion Engineering, Science and Technology).

[18] ASTM G 16 – 95 (Reapproved 2004) Standard Guide for Applying Statistics to Analysis of Corrosion Data.

[19] Knotkova, D., Kreislova, K., Dean, S.W. ISOCORRAG International Atmospheric Exposure Program: Summary of Results, ASTM Series 71, ASTM International, West Conshohocken, PA, 2010.

[20] Tidblad, J., Mikhailov, A. A., Kucera, V. "Application of a Model for Prediction of Atmospheric Corrosion for Tropical Environments". Marine Corrosion in Tropical Environment, ASTM STP 1399, American Society for Testing and Materials, West Conshohocken, PA, 2000.

[21] Mendoza, Antonio R, and Francisco Corvo. "Outdoor and Indoor Atmospheric Corrosion of Non-Ferrous Metals." Corrosion Science 42, no. 7 (July 2000): 1123–1147. doi:10.1016/s0010-938x(99)00135-3.

[22] Tidblad, Johan, Vladimir Kucera, Farid Samie, Surendra N. Das, Chalothorn Bhamornsut, Leong Chow Peng, King Lung So, et al. “Exposure Programme on Atmospheric Corrosion Effects of Acidifying Pollutants in Tropical and Subtropical Climates.” Water, Air, & Soil Pollution: Focus 7, no. 1–3 (January 6, 2007): 241–247. doi:10.1007/s11267-006-9078-6.

[23] Chico, B., D. De la Fuente, J. M. Vega, and M. Morcillo. “Mapas de España de Corrosividad Del Zinc En Atmósferas Rurales.” Revista de Metalurgia 46, no. 6 (December 30, 2010): 485–492. doi:10.3989/revmetalmadrid.1035.

[24] Chen, Wenjuan, Long Hao, Junhua Dong, and Wei Ke. “Effect of Sulphur Dioxide on the Corrosion of a Low Alloy Steel in Simulated Coastal Industrial Atmosphere.” Corrosion Science 83 (June 2014): 155–163. doi:10.1016/j.corsci.2014.02.010.

[25] Zhang, Xu, Shanwu Yang, Wenhua Zhang, Hui Guo, and Xinlai He. “Influence of Outer Rust Layers on Corrosion of Carbon Steel and Weathering Steel During Wet–dry Cycles.” Corrosion Science 82 (May 2014): 165–172. doi:10.1016/j.corsci.2014.01.016.

[26] Castañeda, Abel, Dainerys Fernández, Cecilia Valdés, and Francisco Corvo. "Estudio de la corrosión atmosférica en una zona estratégica de Cuba." Revista CENIC. Ciencias Químicas 46 (2015): 14-25.

[27] Chico, Belén, Daniel De la Fuente, Iván Díaz, Joaquín Simancas, and Manuel Morcillo. "Annual atmospheric corrosion of carbon steel worldwide. An integration of ISOCORRAG, ICP/UNECE and MICAT databases." Materials 10, no. 6 (2017): 601. doi:10.3390/ma10060601.

[28] Surnam, B Y R, and C V Oleti. “Atmospheric Corrosion in Mauritius.” Corrosion Engineering, Science and Technology 47, no. 6 (September 2012): 446–455. doi:10.1179/1743278212y.0000000026.

[29] Araban, V., M. Kahram, and D. Rezakhani. “Evaluation of Copper Atmospheric Corrosion in Different Environments of Iran.” Corrosion Engineering, Science and Technology 51, no. 7 (May 17, 2016): 498–506. doi:10.1080/1478422x.2016.1144265.

[30] Sabir, S., and A. A. Ibrahim. “Influence of Atmospheric Pollution on Corrosion of Materials in Saudi Arabia.” Corrosion Engineering, Science and Technology 52, no. 4 (February 9, 2017): 276–282. doi:10.1080/1478422x.2016.1274839.

[31] Panchenko, Yulia, Andrey Marshakov, Timofey Igonin, Ludmila Nikolaeva, and Victoria Kovtanyuk. “Corrosivity of Atmosphere Toward Structural Metals and Mapping the Continental Russian Territory.” Corrosion Engineering, Science and Technology 54, no. 5 (March 20, 2019): 369–378. doi:10.1080/1478422x.2019.1594526.